Solid-State Film Diffusion for the Production of Integrated Optical Waveguides

D. Kapila and J. L. Plawsky
Chemical Engineering Dept., Rensselaer Polytechnic Institute, Troy, NY 12180

Solid-state film ion exchange (Ag^+-Na^+) in glass substrates has been investigated for the fabrication of passive, integrated, optical waveguides. A new ion exchange mechanism is proposed which couples the oxidation of silver metal to silver oxide and the diffusion of silver ions into the glass substrate. At high electric fields and/or high temperatures, the growth rate of a silver oxide film limits the formation of mobile silver ions and constrains the diffusion of silver into the glass. This new mechanism is able to predict the dopant distribution profile under those conditions and under conditions where a constant surface concentration is appropriate (infinitely thick oxide film). It also explains the characteristics of the current vs. time curve measured during the ion exchange process. The formation and growth of the silver oxide film were confirmed by X-ray photoelectron spectroscopy and X-ray diffraction analysis.

Introduction

For centuries, man has employed light to fuel his scientific and technological development. A marked discontinuity in the pace of this exploitation occurred in 1960 with the demonstration of the laser. It was quickly seen that coherent light from lasers had potential applications in communications, information processing, medicine and surgery, measurement, material processing, and in the general scientific and defense communities. These photonic applications have been aggressively pursued and many, such as optical fiber communications, are now key elements of our technology.

All optical communication systems rely on waveguides or optical fibers for confining and transmitting optical signals over large distances. In the late 19th century, John Tyndall (1820–1893) demonstrated, for the first time, total internal reflection in a water stream. Today, this phenomenon is the basis of all guided-wave optics. Optical fibers or waveguides consist of a core guiding region of high refractive index surrounded by a cladding of a lower refractive index. The optical signal propagates in the core and is confined by total internal reflection at the core-cladding boundary. Two major families of waveguides exist: singlemode and multimode. Single-mode waveguides are characterized by very small core sizes (10 μm), small index differences between the core and cladding regions, and essentially unlimited bandwidth. They are used for long-distance telecommunications and in data communications systems requiring the highest transmission rates. Multimode guides have much larger cores (50 μm), and index differences and consequently much narrower bandwidths. The bandwidth limitations are offset by the ease with which multimode guides can be connected and configured into large-scale local networks.

Early in the development of optical fiber communications, Miller (1969) proposed a miniature form of optical circuitry which held "the possibility of guiding laser beams along miniature transmission lines," where "complex circuit patterns could be defined by photolithographic techniques on planar substrates." Among the advantages claimed for these integrated optical devices were increased isolation from thermal and mechanical disturbances, decreased power dissipation due to the low light levels required to drive the components, and the ability to mass-produce complicated circuits. Using electrooptic or nonlinear optic crystals as the substrates for these waveguides promised the development of low-power optical

Correspondence concerning this article should be addressed to J. L. Plawsky.

modulators and frequency converters for use in communications switches and optical computers.

Today, the art of integrated optics covers a wide range of material technologies, and integrated optical waveguides (IOWs) in glass and crystal substrates are seen as critical to the future development of photonic systems such as optical computers. Ion exchange in glasses and crystals is one important method of fabricating these devices. The ion exchange process has been used to fabricate optoelectronic circuits in crystals such as lithium niobate (Syms, 1988) and to fabricate passive splitting and distribution networks in glasses (Ramaswamy and Srivastava, 1988). Several commercially available devices exist, but the circuits are very expensive, not widely used, and the process is still more of an art than a science. Nearly all current optical waveguide switching and distribution networks use individual optical waveguides and some mechanical means to switch the signals from one channel to another. Considerable space and reliability advantages would be realized if multichannel integrated waveguide components could be fabricated on a monolithic substrate. Moreover, if optical communication technology is to reach the individual, the process for making these integrated circuits must be understood and optimized to produce commodity-priced items.

Ion exchange, which has been used for many years to produce tinted glass, has become one of the methods of choice for the manufacture of integrated waveguides. Since 1972 when Izawa and Nakagome (1972) reported the first ion-exchanged waveguide by exchange of Tl^+ ions in a silicate glass containing oxides of sodium and potassium, significant progress has been made toward understanding the underlying principles of the process. Alkali ion exchange is generally utilized to produce light-guiding structures, since any alteration of the electronic structure of glass or a crystal yields a refractive index change. The introduction of a dopant into the substrate changes the refractive index as a result of two major effects. The first effect is physical and relates to the atomic size of the exchanging ions. If a small ion such as Li^+ replaces a larger ions such as Na^+, the substrate network will collapse around the smaller ion to produce a more densely packed structure that usually has a higher refractive index. The second effect relies on a change in the electronic polarizability of the exchanging ions. If Ag^+, for instance, replaces an ion of smaller polarizability such as Na^+, an increase in the refractive index will also result.

Ion exchange is usually performed in one of the two configurations shown in Figure 1. The first and oldest process can be carried out by immersing the substrate into a molten salt bath containing the ion to be introduced. This process is used to make a wide variety of optical components including the Selfocgraded index lenses used in personal copiers. The second process, a solid-state method, avoids the use of corrosive molten salts by using a thin metal film as the ion source instead. Since diffusion is so slow in glass and crystal substrates, an electric field is usually applied to enhance the ion exchange process.

The exchange of Ag^+ for Na^+ ions in glass has been the most widely explored ion exchange technique (Doremus, 1964; Ramaswamy and Srivastava, 1988; Albert and Lit, 1990; Honkanen et al., 1986). The solid-state film diffusion process has been used by a number of investigators (Najafi et al., 1986; Forrest et al., 1986; Viljanen and Leppihalme, 1980; Kaneko, 1990) and offers several advantages over the molten salt ion

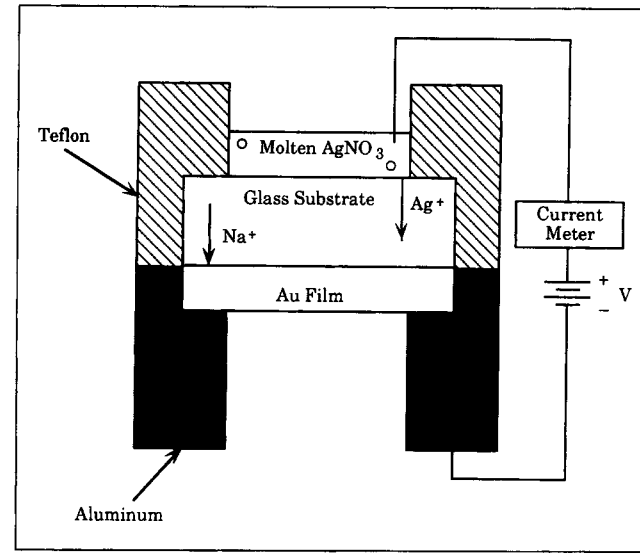

Figure 1a. Molten salt technique for ion-exchange of Ag^+-Na^+.

exchange technique. For instance, the use of very high purity starting materials results in a much cleaner overall process. Waveguide refractive index profiles are more uniform, because the temperature and concentration gradients across the width of the sample are much lower than in the molten salt technique. Waveguides can be fabricated at lower or higher temperatures in the solid-state technique, since one is not constrained by the melting or decomposition points of the salt and low loss waveguides with a large change in refractive index ($\Delta\eta$) can be produced easily without the reduction of silver inside the glass substrate. The solid-state technique does have the disadvantage of not being able to produce deep single-mode waveguides (easily accomplished with the molten salt technique) and the difficulty of producing symmetric refractive index profiles for coupling to conventional optical fibers.

The ion-exchange process in solid-state diffusion is governed by fundamental heat- and mass-transfer mechanisms. Many attempts have been made to model the process (Najafi et al., 1986; Forrest et al., 1986; Albert and Lit, 1990; Ramaswamy

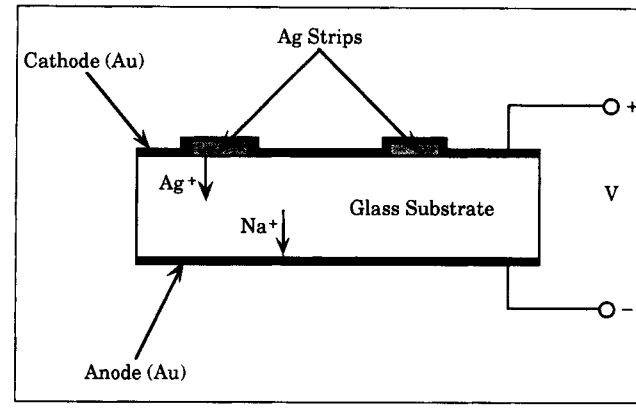

Figure 1b. Solid-state diffusion process for Ag^+-Na^+ exchange.

and Srivastava, 1988; Li and Johnson, 1992). Most investigators have assumed a semiinfinite solid substrate, local electroneutrality during the exchange, and a uniform electric field and temperature across the substrate. In such instances, the governing equation for solid-state film diffusion or molten-salt ion exchange into a glass or crystal substrate is given by:

$$\frac{\partial C_a}{\partial t}=\frac{\partial}{\partial x}\left[\frac{D_a}{\left(1-\alpha\frac{C_a}{C_o}\right)}\frac{\partial C_a}{\partial x}\right]-\left[\frac{\mu}{\left(1-\alpha\frac{C_a}{C_o}\right)}\right]E\frac{\partial C_a}{\partial x} \quad (1)$$

When dilute solutions are assumed (C_a is small compared to C_o) and the mobility of the incoming ion is small compared to the exchanged ion ($\alpha \approx 1$; a good assumption for Ag^+-Na^+ exchange), the governing differential equation may be simplified to:

$$\frac{\partial C_a}{\partial t}=D\frac{\partial^2 C_a}{\partial x^2}-\mu E\frac{\partial C_a}{\partial x} \quad (2)$$

Equation 2 is subject to the boundary conditions:

$$C_a(x,0)=0 \quad x\geq 0 \quad (3a)$$

$$C_a(\infty,t)=0 \quad t\geq 0 \quad (3b)$$

The above partial differential equation has been solved by most authors assuming a constant surface concentration of diffusing ion in addition to the above mentioned boundary conditions:

$$C_a(0,t)=C_o \quad t\geq 0 \quad (4)$$

The solution obtained was (Forrest et al., 1986):

$$C_a(x,t)=\frac{C_o}{2}\left[\exp\left(\frac{\mu Ex}{D}\right)\operatorname{erfc}\left(\frac{x+\mu Et}{2\sqrt{Dt}}\right)+\operatorname{erfc}\left(\frac{x-\mu Et}{2\sqrt{Dt}}\right)\right] \quad (5)$$

Experimentally we have found that at high electric fields and/or high temperatures, Eq. 5 is not able to fully predict the experimental dopant curve. Others, including Forrest et al. (1986), Albert and Lit (1990), and Najafi et al. (1986) have noticed the discrepancy and attributed it to experimental error. The use of Eq. 5 results in an overprediction of the Ag concentration near the surface and underprediction further into the substrate. In addition, strictly linear diffusion coupled to the constant dopant concentration boundary condition is not able to completely explain the experimentally observed variation of the current flow vs. time during the ion-exchange process (Najafi et al., 1986). In particular, Najafi et al. (1986) found that the maximum current flow is related directly to the amount of dopant metal initially deposited on the substrate, and Viljanen and Leppihalme (1981) found that the current always passes through a maximum.

In this article, we propose a new mechanism for solid-state ion exchange which is able to accurately predict the above-mentioned deviations in the dopant concentration profiles. The new mechanism is also able to predict a current vs. time curve similar to the one observed experimentally and explains why the maximum current is related to the amount of dopant metal initially deposited. We derive the new mechanism from mass-transfer fundamentals and show experimental verification of the new model.

Model Development

The departure of the silver concentration profile from the analytical solution, Eq. 5, led us to believe that the constant concentration boundary condition is not justifiable for solid-state film diffusion. As additional evidence, the current measured during the exchange process increases as time proceeds, reaches a maximum, and thereafter decreases until all silver is depleted. Regardless of the amount of silver initially deposited on the substrate, the current vs. time curve always starts out close to zero and passes through a maximum (Najafi et al., 1986), decreasing again until all the silver is absorbed by the glass. Moreover, the maximum current is always related to the amount of silver initially deposited. Transient diffusion coupled to a constant surface concentration boundary condition cannot explain this behavior. Though others have abandoned a constant concentration boundary condition, (Ramaswamy and Srivastava, 1988; Li and Johnson, 1992), these authors were attempting to model a molten-salt system where Ag concentration in the salt was controlled by electrolytic release.

We propose that, for silver or any other metal to diffuse into glass, it has to be oxidized first. The resulting oxide layer, which forms at the interface between the glass and silver metal, acts as the source of Ag^+ ions. Mobile Ag^+ to fuel the exchange process is formed at defect sites in the oxide, and the number of defect sites is a function of the process temperature. Therefore, the thickness of the oxide layer at the interface determines the amount of free Ag^+ available for exchange and hence the characteristics of the silver concentration profile in the glass. In this situation, the flux of silver ions into the substrate is controlled by the amount of silver oxide present at the interface. To determine how much silver oxide exists at the metal-glass interface, we must know the growth kinetics of metal oxide. In the following sections, we borrow from the theory of metal oxidation in air to determine the growth kinetics of silver oxide and postulate an analogy between silver oxidation in the oxidizing mediums—air and glass.

Theory of metal film oxidation

Oxidation Mechanism. Whenever a metal is exposed to an oxidizing medium, there is a thin film of oxidized compound formed which acts as a dielectric or semiconducting barrier layer separating the metal from the medium. Figure 2 shows the formation of an oxide at the interface between a metal and air.

According to Cabrera and Mott (1949), when a film of oxide on the metal is exposed to oxygen, a layer of oxygen is adsorbed on the surface. The adsorbed oxygen captures an electron which tunnels through from the metal (Rehren et al., 1991) and is converted to O^- ion. This establishes an intense electric field ($E=-V/L\cong 10^7$ V/cm) between the metal and the adsorbed oxygen. Electrons pass through the oxide film until a

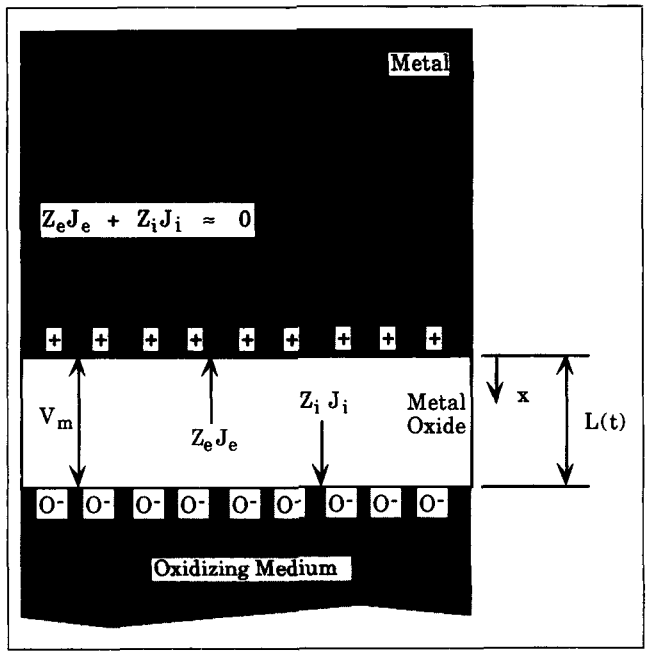

Figure 2. Schematic diagram of oxide formation on metals showing the Mott potential, V_m, and the movement of electrons, J_e, and metal cations, J_i.

quasi-steady state is reached, where the number of electrons passing in either direction is the same. According to Fehlner and Mott (1970), oxides like Ag_2O (structure similar to Cu_2O) form amorphous materials with no open network structure. In their tight, compact, arrangement, the small cations are only weakly bound and there are no large channels available for anion transport. Hence, the cations are expected to move through the metal oxide easily, while the anions are fixed. This phenomenon has been confirmed, using radioactive tracers, for the oxidation of copper to copper oxide. In copper oxidation, the migration of the ions was determined to be activated by the movement of vacant cationic sites (Bardeen et al., 1946). Since silver oxide is very similar in structure to copper oxide and forms the same type of semiconductor, this mechanism should also drive diffusion through the silver oxide film.

The strong electric field set up by the adsorbed O^- ions causes the interstitial cations (metal ions) to be pulled toward the oxygen ions. Every ion which escapes from the metal surface (as a result of a defect) is prevented from recombining with the metal due to the strong electric field. The metal ions form interstitial cations in the oxide film and eventually combine with the adsorbed O^- ions to form more oxide. The transport of cations through the oxide film is such that overall electroneutrality is maintained by an equal and opposite flow of electrons, not anions. The electroneutrality condition for the system is given by:

$$Z_iJ_i + Z_eJ_e = 0 \tag{6}$$

where J_i and J_e are the ionic and electronic current densities, respectively.

We propose that a similar mechanism of silver oxidation occurs when the gaseous oxidizing medium is replaced by a solid-oxidizing medium like glass (when molten, glass is one of the most potent oxidizing solvents known). Glass, especially at the metal-glass interface, has a number of nonbridging oxygen ions formed by the addition of alkali oxide constituents and by defects due to strained surface bonds. These inherent O^- ions perform the same function as the adsorbed O^- ions of the Cabrera-Mott mechanism. They establish the required electric field to pull the metal ions into the oxide film from the metal surface.

A simple, field-assisted, linear, diffusion mechanism cannot be used to describe the metal oxidation process because:

a) The electric field established is high and so the drift velocity of the cation is no longer linearly proportional to the electric field (as in the case of linear, field-assisted diffusion).

b) There are several electron transport mechanisms including tunneling, thermionic emission, diffusion, and electrical conduction, which may be operative during oxidation process. Some of these mechanisms do not strictly obey Fick's law.

c) The electric field driving the formation of metal oxide cannot be considered constant over time (Fromhold, 1976).

Growth Rate Kinetics. Of the various electron transport mechanisms (electron tunneling, thermionic emission, diffusion, and electrical conduction) operative in thin-film, low-temperature (<650°C), oxidation, transport due to electron tunneling, is predominant. The growth rate of the metal oxide can be controlled by the flux of electrons or the flux of cations across the metal oxide barrier layer. If the metal oxide film is thin, one can assume that the effect of any space charge is negligible (see Eq. 6), and so the motion of the cations and electrons can be considered independently. Initially, for very thin oxides, the electric field across the oxide is extremely high. The electrons are freely able to penetrate the thin oxide film by tunneling. Hence, the rate of metal oxide growth is limited by the flux of the diffusing cations. As the thickness of the film grows, the electrons find it progressively more and more difficult to tunnel across the oxide film. To maintain overall electroneutrality, the potential drop across the oxide film begins to decrease (limiting the flux of cations), and so the flux of electrons eventually becomes the rate-limiting step. At this stage, the current flow across the oxide reaches an asymptotic value and so does the metal oxide film thickness.

The growth rate of the oxide film can be expressed in terms of the rate-controlling current density, J_c:

$$\frac{dL}{dt} = R_cJ_c(L) \tag{7}$$

where J_c is the smaller of the two currents, J_i and J_e. R_c is the volume of oxide formed per particle of the rate-limiting species which reaches the oxide-oxygen interface.

Fromhold (1976) analyzed metal oxidation considering the two rate-limiting factors: electron transport by tunneling and cation migration. According to his "Hopping model for ionic diffusion in large surface charge field" (Fromhold, 1976), the diffusing cation must overcome a number of potential barriers in the oxide network to reach the oxidizing surface. The height of the potential barrier is modified by the electric field established by the adsorbed oxygen ions. In the homogeneous-field limit, where all space charge contributions to the field are neglected relative to the surface-charge field E_o (very realistic for thin silver oxide films), Fromhold derived the following expression for ionic diffusion current J_i:

$$J_i = 4a\nu_i \exp\left(\frac{-W_i}{k_B T}\right)\sinh\left(\frac{Z_i e E_o a}{k_B T}\right) \times \left[\frac{C_i(L) - C_i(0)\exp\left(\frac{Z_i e E_o L(t)}{k_B T}\right)}{1-\exp\left(\frac{Z_i e E_o L(t)}{k_B T}\right)}\right] \quad (8)$$

The parameters $C_i(L)$ and $C_i(0)$ are the bulk concentrations of the diffusing ionic species (Ag^+) at the oxide-glass interface ($x=L$) and at the metal-oxide interface ($x=0$), respectively. $Z_i e$ is the effective charge per particle of the ionic species (Ag^+) transporting through the lattice, W_i is the thermal activation energy for ionic motion, a is the half ionic jump distance, and ν_i is the ionic vibration frequency. For silver oxidation, $Z_i e$ is a positive unit electric charge. We also know that in the case of silver oxidation, $E_o(-V/L)$ is positive (Cabrera and Mott, 1949; Rehren et al., 1991), $C_i(0) > C_i(L)$ for diffusing cation interstitials (Ag^+), and Z_i is also positive. [A very rough numerical estimate of V is given by: $eV = E + W_{\text{bind}} - \phi_o$, where ϕ_o is the work function of silver against vacuum ($\cong 4.7$ eV), E is the electron affinity of 0 (≈ 2.2 eV), and W_{bind} the adsorption energy of an oxygen ion O^- on the surface of oxide (≈ 1.0 eV). From these values, we get $V \cong -1.5$ V.] The exponential term in Eq. 8 is very large for silver oxidation, and so J_i reduces to an expression first proposed by Cabrera and Mott (1949).

$$J_i \cong 4a\nu_i C_i(0)\exp\left(\frac{-W_i}{k_B T}\right)\sinh\left(\frac{Z_i e E_o a}{k_B T}\right) \quad (9)$$

where $E_o = -V_m/L$ and V_m is the Mott potential (caused by oxygen ions) across the growing oxide film.

Using fundamental quantum physics principles, Fromhold (1976) derived the following expression for the net electron tunneling current in the oxide film:

$$J_e = \frac{1}{8\pi^2 \hbar L^2}[\{2\chi_o - eV_K\}\exp\{-2m^{1/2}\hbar^{-1}L(2\chi_o - eV_K)^{1/2}\} - \{2\chi_L + eV_K\}\exp\{-2m^{1/2}\hbar^{-1}L(2\chi_L + eV_K)^{1/2}\}] \quad (10)$$

Here, $V_K = -E_o L(t)$ is the total electrostatic potential across the oxide film (similar to the Mott potential, V_m), m is the mass of the electron, χ_o is the metal-oxide electron work function, and χ_L is the O^--oxide work function. Whether the film growth rate is controlled by electron tunneling or cation migration, the rate is a function of the film thickness and decreases as the film thickness increases.

Equations 6, 7, 9 and 10 are used in the numerical calculation of the oxide growth rate. At the start of the integration, J_c is equal to the ionic diffusion current density, J_i, and remains equal to J_i until the value of V_K approaches the ionic equilibrium potential $V_{\text{Eq}} = -E_{\max} L(t)$. Here, $E_{\max}$ is the largest field which can be created by diffusing ionic species and which yields a zero value for the ionic current, J_i.

$$E_{\max} = \left[\frac{k_B T}{Z_i e L(t)}\right]\ln\left(\frac{C_i(L)}{C_i(0)}\right) \quad (11)$$

when $E_o = E_{\max}$ the value of J_i becomes zero. The net ionic current is very small compared to the forward ionic current due to the concentration gradient or the reverse current due to the imposed electric field (drift). At this point, oxide growth is no longer ionic-current-limited, it is electronic tunneling-current-limited, and J_c is taken to be the electronic current, J_e. The integration proceeds until a limiting oxide thickness is reached.

The simultaneous numerical solution of Eqs. 6, 7, 9, 10 leads to an oxide growth curve which can be empirically fitted to direct (or inverse) logarithmic function (unlike the parabolic growth rate curve obtained, assuming the validity of the linear field assisted diffusion equation). It has been observed experimentally that the oxidation of silver in air follows a logarithmic growth rate of this form (Kubaschewski and Hopkins, 1962)

$$L(t) = a' \log(bt + 1) \quad (12)$$

Coupled oxidation and diffusion

We propose that in solid-state, field-assisted film diffusion, the oxide substrate acts as the oxidizing medium instead of air. The film growth rate is related to Eq. 7, but now must be modified for the effect of the applied electric field. In presence of an applied electric field $E_o = -(V_m + V_{\text{ox}})/L$, where V_{ox} is the potential across the oxide due to the applied electric field. In solid-state-film ion exchanges, $V_{\text{ox}} \ll V_m$, hence $E_o \approx -V_m/L$. Due to the presence of an applied electric field, the current due to ionic and electronic particles is:

$$\frac{I}{FA} = Z_i J_i + Z_e J_e \quad (13)$$

where I is the current flow due to the applied electric field, F is Faraday's constant, and A is the electrode area. The current density (I/A) is usually small compared to the individual particle currents, and so Eq. 13 can be approximated as:

$$Z_i J_i + Z_e J_e \approx 0 \quad (14)$$

The growth rate curve must also be modified by a term describing the decrease in film thickness due to the flux of Ag^+ into the substrate. Unlike air, the substrate acts as both an oxidizing medium and a sink for the oxidized metal. Assuming dilute solutions, we can write the modified growth rate as:

$$\frac{dL}{dt} = R_c J_c(L) - \frac{Mw_{Ag_2O}}{\rho_{Ag_2O}} J_{Ag}(0,t) \quad (15)$$

where J_{Ag} is the silver flux into the oxidizing medium, ρ_{Ag_2O} is the density of silver oxide, and Mw_{Ag_2O} is the molecular weight of silver oxide. Numerical integration of this equation with growth rate limitations coming from cation migration followed by electron tunneling still leads to logarithmic growth kinetics following Eq. 12, but with different growth rate parameters, a' and b. As the silver flux entering the substrate increases under the application of an external electric field, the oxide film thickness decreases. The oxide thickness can never be depleted, because the growth rate is inversely proportional to the film thickness. This always ensures that there will be silver

oxide on the surface for diffusion to proceed (limited by the amount of silver metal initially deposited).

To model the solid-state diffusion process, we do not use Eq. 5 as the description of the concentration profile within the substrate, but consider a slightly different formulation. We look at the diffusion of a finite quantity of silver, M, into the semiinfinite structure under the application of an electric field. The mass of mobile silver ions, M, is proportional to the thickness of the oxide film $[L(t)]$, hence M is a function of time defined by Eq. 14 and the density of silver oxide $[M \propto \rho_{Ag_2O} * A * L(t)]$. The density of the oxide formed in thin oxide films is constant, that is, no compaction or flaking of the oxide takes place. Therefore, M can be approximated by a logarithmic function of the form of Eq. 12. The Ag^+ concentration profile in the glass is given by the fundamental source solution (Crank, 1956):

$$C_a(x,t) = \frac{M}{\sqrt{\pi D t}} \exp\left(-\frac{[x-\mu E t]^2}{4Dt}\right) \tag{16}$$

which describes the spreading by field-assisted diffusion of an amount of substance M deposited at time $t=0$ in the plane $x=0$. Since M is a function of time, we obtain the final dopant profile (in the presence of an electric field) in the substrate by superposition of the plane source solution over time and oxide layer thickness.

$$C_a(x,t) = \frac{\rho_{Ag_2O}}{Mw_{Ag_2O}} \int_0^t \int_x^{x+L} \exp\left\{-\frac{[x-x'-\mu E(t-t')]^2}{4D(t-t')}\right\} dx'\, dt' \tag{17}$$

We have used the numerical solution of Eq. 17 in combination with the logarithmic growth kinetics (Eq. 12) for the oxide film to fit experimentally obtained silver concentration profiles in glass substrates.

Experimental Procedures

Waveguide fabrication

The Ag diffusion experiments were run using 1-mm-thick Fisher Brand (cat #12-550C), glass slides and a proprietary Corning glass developed specifically for ion exchange. The composition of the Fisher Brand glass is given in Table 1. The substrates were cleaned carefully following a standard RCA cleaning procedure. They were first immersed in a hot mixture of ammonium hydroxide, hydrogen peroxide and deionized water in a ratio of 1:1:5 to remove any organic residues. This was followed by a deionized water rinse and then immersion in dilute hydrofluoric acid to remove any metallic impurities and a thin layer of glass. A final rinse in deionized water prepared the samples for metal deposition. A thick Ag layer (≈ 1.5 μm) was evaporated on one face of the glass sample. On top of the silver layer, a 0.2-μm-thick layer of gold was evaporated to act as an anode. On the other face of the glass sample, another 0.2-μm-thick layer of gold was evaporated to act as an inert cathode. Gold electrodes were used because they resist corrosion from the precipitating sodium and create a uniform distribution of electric field across the sample face as the silver film diffused into the glass. Since gold readily diffuses into silver, concern about changes in the dopant source concentration arose. Fortunately, XPS scans of the dopant metal film after diffusion indicated that gold diffusion into silver was negligible within the time scales of the experiments performed (<2 h). The substrate samples, as prepared by the above procedure, were put into a furnace with an applied electric field to enhance the ion exchange process. The diffusion process was stopped well before the silver film was depleted to avoid any spatial inhomogeneities which might occur during the diffusion.

Table 1. Composition of Soda Lime Silicate Glass (Fisher Brand 12-550C)

Chemical Constituent	Wt. %
SiO_2	72.26
Na_2O	14.31
K_2O	1.2
CaO	6.4
MgO	4.3
Al_2O_3	1.2
Fe_2O_3	0.03
SO_3	0.3

Ag profile characterization

After the ion-exchange process the glass samples were taken out of the furnace, and the remaining gold-silver films were removed from the anode and the cathode. The volume occupied by silver oxide is approximately 1.6 times the volume occupied by silver metal. The stresses resulting from the volume expansion facilitate the removal of the dopant film from the glass substrate. At the opposite end, sodium plates out on the gold cathode make removal of the cathode very easy as well. The glass samples were cleaved using a diamond knife and cemented together, edge up for subsequent analysis. The cemented samples were polished across the edge of the waveguide. The depth profile of silver ions in glass was obtained by detecting the back-scattered electrons, when the sample was bombarded by high-energy (10 kV) electrons in a JEOL 733 electron microprobe (Ramaswamy and Najafi, 1986). Since the silver atoms have a higher atomic weight, contribution of the silver ions to the yield of back-scattered electrons is much higher than that of other glass constituents. The polished glass samples were coated with a thin layer of carbon to avoid charge buildup during the electron beam scanning. The back-scattered electrons can be produced by silver ions as well as reduced silver metal in the glass. The presence of reduced metal indicates supersaturation of the glass and failure of the diffusion process to produce a successful, low-loss waveguide. The possibility of the back-scattered electrons coming from the reduced silver atoms, in addition to Ag^+ ions in any of our experimental glass samples, was ruled out by UV/VIS spectrophotometer scans, which did not show the characteristic metallic silver absorption peak at ≈ 410 nm.

Results and Discussion

Metal oxide presence

Following the ion exchange process, the silver film, on removal from the glass substrate, had a yellowish/dull white

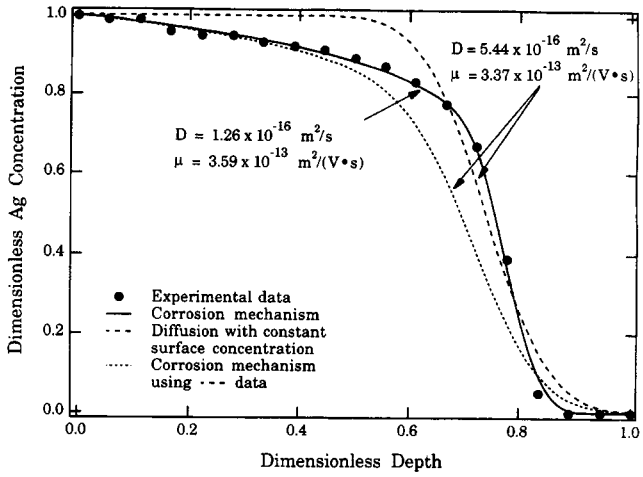

Figure 3. Diffusion with a constant surface concentration boundary condition vs. Ag corrosion mechanism for Ag^+-Na^+ exchange.

Substrate is a Fisher Brand soda-lime-silicate glass. ($T = 327°C$; $E = 200$ V/cm).

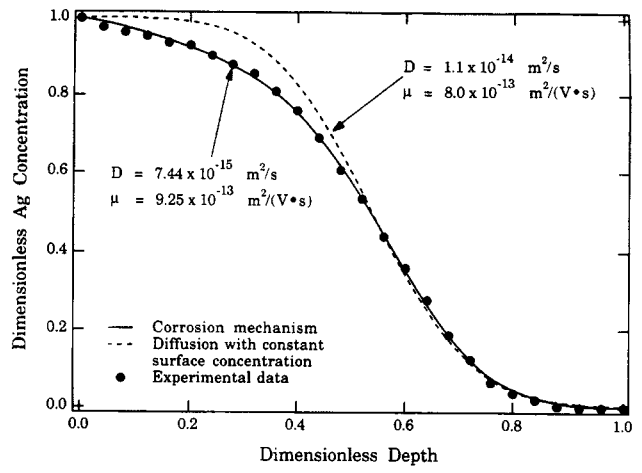

Figure 4. Diffusion with a constant surface concentration boundary condition vs. Ag corrosion mechanism for Ag^+-Na^+ exchange.

Substrate is a proprietary Corning glass ($T = 300°C$; $E = 100$ V/cm).

color in reflected light. The presence and growth of a silver oxide film between the metal and glass substrate were confirmed by X-ray photoelectron spectroscopy (XPS). Small-angle X-ray diffraction data reconfirmed the XPS findings and indicated the presence of a nonstochiometric silver oxide ($Ag_{2-x}O$) at the metal-glass interface.

Dopant profiles

Equation 17 was solved on *Vax/Vms* mainframe using the optimization routine NPSOL to determine the optimum values for the diffusivity, mobility and film growth rate parameter, *b* (see Eq. 12). Figure 3 shows the results of the optimization for a sample processed at a temperature of 327°C and an electric field of 200 V/cm. The solution is compared to the dopant curve obtained using the same optimization routine to fit the data to a constant surface concentration model. The substrate was a Fisher Brand microscope glass. It can be seen that the dopant profile based on the new corrosion mechanism fits the experimental data much better than diffusion with a constant concentration boundary condition. The values of the diffusivity and mobility calculated using the constant concentration condition are close to published values for this type of glass (Chartier et al., 1978; Forrest et al., 1986). These literature values are based on a constant surface concentration curve fit and, in light of the new mechanism, may not be as accurate as once thought. The diffusivity calculated using the corrosion mechanism is smaller than the constant concentration boundary condition and probably a more accurate value. The tail of the experimental dopant profile is steeper in slope than what one would calculate if the surface concentration were constant, and this supports the smaller diffusivity derived from the corrosion model. The mobility calculated using the corrosion mechanism is higher than that obtained using a constant concentration boundary condition. The knee of the experimental dopant profile extends further into the substrate than the constant concentration curve fit, and this also supports the corrosion mechanism's higher mobility value.

The final curve shown in Figure 3 uses the transport properties (diffusivity and mobility) obtained from the constant concentration curve fit in the corrosion mechanism. The growth rate parameter, *b*, remains unchanged. This curve shows the sensitivity of the corrosion mechanism model to the values of the transport parameters.

A set of similar ion exchange experiments was carried out on a proprietary Corning glass. The Corning glass contains high field strength ions, such as Al^{+3}, added to remove the energetic nonbridging oxygen atoms present in most alkali-silicate glasses. Removing these oxygens prevents silver reduction (Araujo, 1992) during the ion exchange by tying up any free electrons associated with the oxygen ions. Hence, in this glass, one can replace every alkali atom by silver without reducing the silver. This glass presents a fundamentally different environment for diffusion from the Fisher Brand glass. The Fisher Brand glass has a number of nonbridging oxygens and can accommodate a limited amount of silver before reduction. Figure 4 shows the results of the optimization for a Corning sample processed at a temperature of 300°C and a low electric field of 100 V/cm. The solution is compared to the dopant curve obtained by assuming a constant surface concentration boundary condition. As can be seen from the figure, the Corning glass, even though compositionally quite different from the generic soda lime microscope glass, exhibits the same trends in the dopant profile and the same mechanism of ion exchange, the corrosion mechanism, fits the data with excellent precision. The corrosion mechanism derived diffusivity is smaller than the diffusivity calculated using diffusion with constant surface concentration, and the mobility calculated based on the corrosion mechanism is higher. This is in agreement with the results obtained using the Fisher Brand soda-lime-silicate glass. These trends are not as clear as those observed in the soda-lime-silicate glass due to the lower electric field assist. However, the experimental dopant curve clearly exhibits an initial slope inconsistent with diffusion using a constant surface concentration boundary condition.

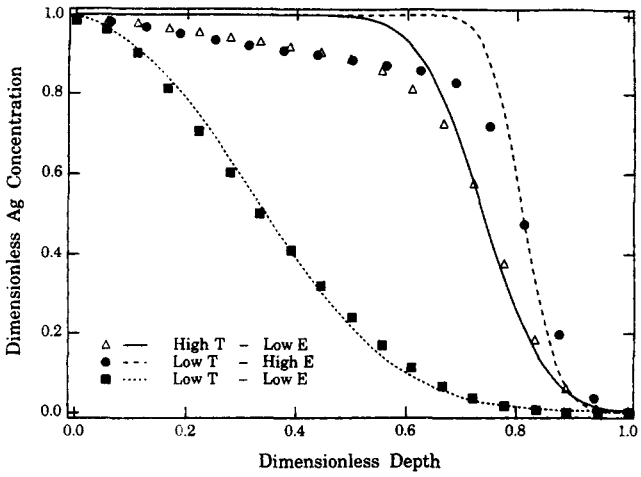

Figure 5. Ag^+ diffusion control vs. film growth rate control during solid-state film diffusion in Fisher Brand soda-lime-silicate glass.

Markers represent experimental data. Lines are curve fits using a constant surface concentration boundary condition.

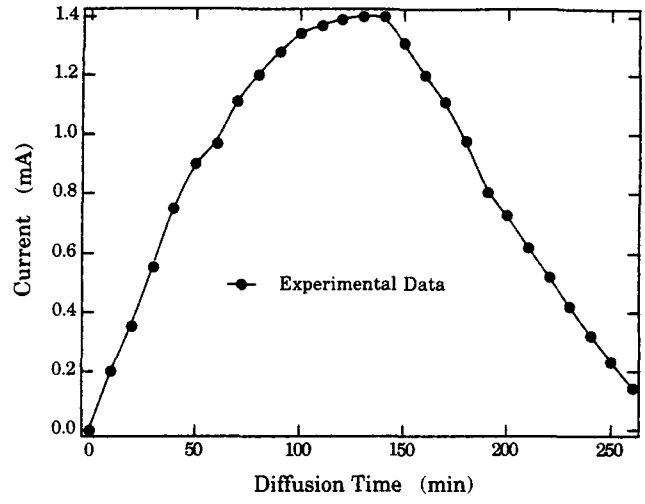

Figure 6. Current variation with time for solid-state Ag film diffusion in Fisher Brand soda-lime-silicate glass.

($T = 275°C$; $E = 160$ V/cm).

During the course of our experiments, we have also observed that the regime of mass transfer depends on the diffusion temperature and the electric field strength. At low temperature and moderate electric field strengths ($T = 245°C$, $E = 400$ V/cm), the Ag doping process is diffusion-limited, as shown in Figure 5. Under these conditions, the oxide film growth rate is much faster than the external flux, and so the oxide layer appears to be infinite in extent. A constant concentration boundary condition can be used, and the experimental dopant profile is indistinguishable from a classic error function profile. The corrosion model based on Eq. 17 produces an error function profile when the film thickness is very large, $L \to \infty$. At low temperature and higher electric field ($T = 225°C$, $E = 600$ V/cm), the doping process becomes oxide-film-growth-rate-controlled. Here, the film growth rate is very slow and so the substrate does not see an infinite oxide layer. The error function profile is no longer applicable, and the flux into the substrate is controlled by the amount of mobile Ag^+ ions available for exchange and hence by the oxide layer thickness. Finally, at high temperatures and any electric field strength ($T = 327°C$, $E = 200$ V/cm), the doping process becomes totally oxide-film-growth-rate-controlled. Here, the diffusivity and mobility of the dopant are very high, the film growth rate is low, and the amount of dopant in the glass is again controlled by the formation and extent of the silver oxide film.

Current variation

The current vs. time curve in Figure 6 was obtained for solid-state film diffusion where the Ag^+ flux never reached a pseudo-steady state due to an insufficient thickness of deposited silver metal. This phenomenon of a sharp peak in the current vs. time curve has also been observed by other investigators (Najafi et al., 1986). The variation in current as a function of time in Figure 6 can be explained by the corrosion mechanism. The mechanism also explains Najafi et al.'s observation that the maximum current increases with increasing deposition of silver metal.

Integrating the current vs. time curve allows to estimate that, if there is insufficient silver metal to reach a pseudo-steady current during the diffusion, the peak of the curve corresponds to the point at which all the silver in the film is converted to silver oxide. We refer to this point as breakthrough. An XPS analysis of the deposited dopant films showed that, as diffusion progresses, the thickness of the silver oxide layer grows. As the thickness of the deposited Ag metal film is increased, the silver oxide thickness at the metal-glass interface will increase at breakthrough and so the maximum current will increase. Beyond breakthrough, the current decreases because the thickness of the oxide film decreases. If sufficient amount of silver metal is deposited, the current will eventually reach a maximum corresponding to the point at which the film growth rate is zero ($dL/dt = 0$, Eq. 15). Beyond this maximum, the current will decrease slightly, because the mobility of silver in the glass is smaller than that of sodium, causing the overall conductivity of the glass to decrease during the exchange. This slow decrease in current as a function of time has been quantified by Viljanen and Leppihalme (1981):

$$\frac{di}{dt} = \frac{i^2}{Fcd}\left(\frac{\sigma_{Na}}{\sigma_{Ag}} - 1\right) \tag{18}$$

σ_{Na} and σ_{Ag} are the conductivities in the unexchanged and exchanged parts of the glass. This decrease in conductivity will occur until breakthrough takes place, whereupon a sharp decrease in current will be observed.

The maximum current has also been found to be linearly related to the applied voltage (Najafi et al., 1986). In our model, this behavior is also accounted for because the film growth rate and hence the current (see Eq. 13) depend on the flux of Ag^+ into the glass, which in turn depends linearly on the voltage dropped across the substrate ($J_{Ag} \propto dC_a/dx$, dV/dx).

Conclusions

We proposed a new corrosion mechanism for fabrication of optical waveguides via solid-state film diffusion. The new mechanism is derived from basic mass-transfer principles governing the oxidation of metals. The process of ion exchange in glass is coupled with the oxidation of silver metal to silver oxide. The presence and growth of oxide were confirmed by XPS analysis and small-angle X-ray diffraction. The oxidation of silver is shown to have a direct logarithmic (or inverse logarithmic) growth rate. The exchange mechanism due to the coupling of oxidation and diffusion is able to predict the observed deviations in dopant curves at high electric field and/or high temperature. It also explains the observed maxima in the current vs. time curve and the dependence of those maxima on the amount of silver metal initially deposited on the substrate.

The corrosion mechanism for solid-state diffusion does not appear to be limited to silver on glass. Copper oxidation follows a similar mechanism to silver, and oxidation and diffusion of copper on glass should exhibit the same behavior as silver and be described by the same model. Any material with sufficient defects to allow oxidation of a metal at the surface should have its solid-state diffusion process described by Eq. 17. This includes Ni or *V* diffusion in $LiNbO_3$ or $KTiPO_4$ for forming electrooptic or optically nonlinear devices, and the recently announced technique of solid-state diffusion of *Er* in $LiNbO_3$ or glass for producing fiber amplifiers (Aboueleil et al., 1991; Brinkman et al., 1991; Becker et al., 1992).

Acknowledgment

The authors would like to express their appreciation to the National Science Foundation under grant CTS-9009481, the Howard P. Isermann Department of Chemical Engineering and the Engineering School of Rensselaer Polytechnic Institute for their encouragement and support of this work.

Notation

a = half ionic jump distance, m
a' = oxide growth rate curve parameter, m
A = area of ion exchange, m^2
b = oxide growth rate curve parameter, s^{-1}
c = sodium concentration, $kmol \cdot m^{-3}$
C_a = concentration of species a, $kmol \cdot m^{-3}$
$C_i(0)$ = ionic-defect concentration at the metal-oxide interface, $C \cdot m^{-3}$
$C_i(L)$ = ionic-defect concentration at the oxide-oxygen interface, $C \cdot m^{-3}$
C_o = initial concentration of ions to be exchanged in the substrate, $kmol \cdot m^{-3}$
d = thickness of glass substrate, m
D, D_a = diffusivity, $m^2 \cdot s^{-1}$
e = unit electron charge, C
E, E_o = electric field, $V \cdot m^{-1}$
E_{max} = maximum electric field created by the diffusing ionic species, $V \cdot m^{-1}$
$\hbar$ = (Planck's constant)/(2π), $J \cdot s$
F = Faraday's constant, $C \cdot kmol^{-1}$
i = current density, $A \cdot m^{-2}$
I = current, A
J_{Ag} = silver ion flux in glass, $kmol \cdot m^{-2} \cdot s^{-1}$
J_c = rate limiting diffusion current density, $C \cdot m^{-2} \cdot s^{-1}$
J_e = electronic diffusion current density, $C \cdot m^{-2} \cdot s^{-1}$
J_i = ionic diffusion current density, $C \cdot m^{-2} \cdot s^{-1}$
k_B = Boltzmann's constant, $eV \cdot K^{-1}$
L = thickness of oxide, m
m = mass of the electron, kg
M = mass of mobile silver ions, kg
Mw = molecular weight kg/kmol
R = oxide volume increase per transported ion, m^3
R_c = oxide volume increase per particle of the rate-limiting species which reaches the oxide-oxygen interface, $m^3 \cdot C^{-1}$
t, t' = time, s
T = temperature, K
V_{Eq} = ionic equilibrium potential, V
V_K = electrostatic potential across the oxide film, V
V_m = Mott potential, V
V_{ox} = potential across the oxide layer due to the applied electric field, V
W_i = thermal activation energy for ionic motion, eV
x, x' = distance, m
Z_e = ratio of diffusing electronic-defect effective charge to electronic charge magnitude, e
Z_i = ratio of diffusing ionic-defect effective charge to electronic charge magnitude, e

Greek letters

α = 1-the ratio of the mobilities of the exchanging ions
χ_o = metal-oxide electron work function, eV
χ_L = O^--oxide work function, eV
μ = mobility, $m^2 \cdot s^{-1} \cdot V^{-1}$
ν_i = ionic vibration frequency, s^{-1}
ρ_{Ag_2O} = silver oxide density, $kg \cdot m^{-3}$
σ_{Na} = conductivity in the unexchanged part of the glass, $ohm^{-1} \cdot m^{-1}$
σ_{Ag} = conductivity in the exchanged part of the glass, $ohm^{-1} \cdot m^{-1}$

Literature Cited

Aboueleil, M. M., G. A. Ball, W. L. Nighan, and D. J. Opal, "Low-Loss Erbium-Doped Ion-Exchanged Channel Waveguides," *Optics Lett.*, **16**, 1949 (1991).

Albert, J., and J. W. Y. Lit, "Full Modeling of Field-Assisted Ion Exchange for Graded Index Buried Channel Optical Waveguides," *Appl. Optics*, **29**, 2798 (1990).

Araujo, R., "Colorless Glasses Containing Ion-Exchanged Silver," *Appl. Optics*, **31**, 5221 (1992).

Cabrera, N., and N. F. Mott, "Theory of Oxidation of Metals," *Rept. Prog. Phys.*, **12**, 163 (1949).

Bardeen, J., W. H. Brattain, and W. Shockley, "Investigation of Oxidation of Copper by Use of Radioactive Cu Tracer," *J. Chem. Phys.*, **14**, 714 (1946).

Becker, P., R. Brinkmann, M. Dinand, W. Sohler, and H. Suche, "Er-Diffused Ti:$LiNbO_3$ Waveguide Laser of 1563 and 1576 nm Emission Wavelengths," *Appl. Phys. Lett.*, **61**, 1257 (1992).

Brinkman, B., W. Sohler, and H. Suche, "Continuous-Wave Erbium-Diffused $LiNbO_3$ Waveguide Laser," *Elec. Lett.*, **27**, 415 (1991).

Chartier, G. H., P. Jaussaud, A. D. D. Oliveria, and O. Parriaux, "Optical Waveguides Fabricated by Electric-Field Controlled Ion Exchange in Glass," *Elec. Lett.*, **14**, 132 (1978).

Crank, J., *The Mathematics of Diffusion*, Oxford University Press (1956).

Doremus, R. H., "Exchange and Diffusion of Ions in Glass," *J. Phys. Chem.*, **68**, 2212 (1964).

Fehlner, F. P., and N. F. Mott, "Low-Temperature Oxidation," *Oxid. Met.*, **2**, 59 (1970).

Forrest, K., S. J. Pagano, and W. Viehmann, "Channel Waveguides in Glass via Silver-Sodium Field-Assisted Ion Exchange," *IEEE J. Lightwave Tech.*, **LT-4**, 140 (1986).

Fromhold, A. T., Jr., *Theory of Metal Oxidation: I. Fundamentals, Defects in Crystalline Solids*, North-Holland Publishing (1976).

Honkanen, S., A. Tervonen, H. V. Bagh, and M. Leppihalme, "Ion Exchange Process for Fabrication of Waveguide Couplers for Fiber Optic Sensor Applications," *J. Appl. Phys.*, **61**, 52 (1986).

Izawa, T., and H. Nakagone, "Optical Waveguide Formed by Electrically Induced Migration of Ions in Glass Plates," *Appl. Phys. Lett.*, **21**, 584 (1972).

Kaneko, T., "The Field Assisted Penetration of a Silver-Film into Glass," *J. Non-Crystalline Solids*, **120**, 188 (1990).
Kubaschewski, O., and B. E. Hopkins, *Oxidation of Metals and Alloys*, Academic Press, New York (1962).
Li, X., and P. F. Johnson, "A General Analytical Solution for the Concentration Profiles of Ion-Exchanged Planar Waveguides," *Mat. Res. Soc. Symp. Proc.*, **244**, 357 (1992).
Miller, S. E., "Integrated Optics: An Introduction," *Bell Syst. Tech. J.*, **48**, 2059 (1969).
Najafi, S. I., P. G. Suchoski, and R. V. Ramaswamy, "Silver Film-Diffused Glass Waveguides: Diffusion Process and Optical Properties," *IEEE J. Quantum Electron.*, **QE-22**, 2213 (1986).
Ramaswamy, R. V., and S. I. Najafi, "Planar, Buried, Ion-Exchanged Glass Waveguides: Diffusion Characteristics," *IEEE J. Quantum Electron.*, **QE-22**, 883 (1986).
Ramaswamy, R. V., and R. Srivastava, "Ion-Exchanged Glass Waveguides: A Review," *IEEE J. Lightwave Tech.*, **6**, 984 (1988).
Ramaswamy, R. V., H. C. Cheng, and R. Srivastava, "Process Optimization of Buried Ag^+-Na^+ Ion-Exchanged Waveguides: Theory and Experiment," *Appl. Optics*, **27**, 1814 (1988).
Rehren, C., M. Muhler, X. Bao, R. Schlogl, and G. Ertl, "The Interaction of Silver with Oxygen: An Investigation with Thermal Desorption and Photoelectron Spectroscopy," *Z. Physikalische Chemie*, **174**, 11 (1991).
Syms, R. A., "Advances in Channel Waveguide Lithium Niobate Integrated Optics," *Optics and Quant. Elect.*, **20**, 189 (1988).
Viljanen, J., and M. Leppihalme, "Fabrication of Optical Waveguides with Nearly Circular Cross Section by Silver Ion Migration Technique," *J. Appl. Phys.*, **51**, 3563 (1980).
Viljanen, J., and M. Leppihalme, "Analysis of Loss in Ion Exchanged Waveguides," Euro. Conf. on Integrated Optics, Institute of Electrical Engineers, London (1981).

Manuscript received Feb. 1, 1993, and revision received Apr. 26, 1993.